

# 南京理工大学

## 本科生课程考查

课程名称： 光学中的计算方法

考试形式： ☐ 专题研究报告      ☒ 课程论文      ☐ 大作业

☐ 综合考试

学生姓名： 邓浩      学号： 9211160D0415

评阅人： 王清华

时 间： 2024 年 6 月

# Partial Coherence Simulation Based on MATLAB

Deng Hao

(Nanjing University of Science & Technology, 210094, China)

**Abstract:** Coherence refers to the amount of correlation in the optical field at separate times or separate points within a beam of light. As the emphasis here is the propagation of partially coherent light, it is constructive to note that generalized analytic solutions exist for the propagation of nonmonochromatic light. The math, however, will be tedious and not intuitionistic.

In this paper, the computation approaches presented are not derived from an analytic solution, but represent a practical strategy based on the concept that partially coherent light is a superposition of irradiance from uncorrelated coherent waves. The simulation of partial temporal coherence and partial spatial coherence is handled in separate ways<sup>1-2</sup>. However, the approaches have the common theme that a series of propagations or imaging simulations are performed using the coherent methods, and then the irradiance patterns from coherent results are summed to give the partially coherent result.

**Key Words:** partial temporal coherence, partial spatial coherence, optical simulation

## 1 Introduction

Optical coherence theory is a rich statistical discipline<sup>3-7</sup>, but in this paper only a few summary results are provided that are specific to the computational discussion.

High coherence leads to stationary interference effects such as the “fringing” and “ringing” structures that appeared in the simulated diffraction and imaging results for monochromatic (coherent) light. These kinds of features are absent from the incoherent imaging results. Coherence is exploited in a variety of optical applications: holography, interferometry, optical coherence tomography, coherent lidar, Fourier transform spectroscopy, and quantum communications, to name a few. Some applications simply require high coherence (holography) while others also take advantage of the lack of coherence (optical coherence tomography). Sometimes coherence is a noise source—such as speckled coherent images.

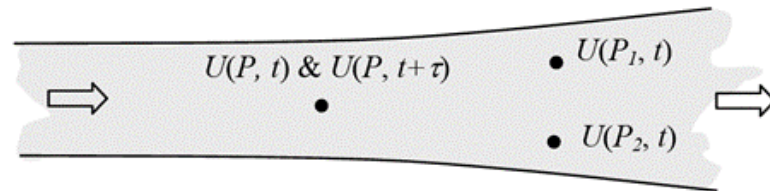


**Figure 1.1** Correlation of complex fields at point P separated in time by  $\tau$  is a measure of temporal coherence. Correlation of fields at points  $P_1$  and  $P_2$  at the same time is a measure of spatial coherence.

It is convenient to separate coherence into two categories: temporal and spatial.

Temporal coherence refers to the correlation (time average of the products of complex fields) at spatial point P but separated in time by  $\tau$ . The degree of coherence for a partial temporal coherent source changes with  $\tau$ , typically, decreasing as  $\tau$  increases. Spatial coherence refers to the correlation of complex fields at the same time but at different transverse points  $P_1$  and  $P_2$ . For a partial spatial coherent source, the degree of coherence typically decreases with separation distance.

## 2 Partial Temporal Coherence

### 2.1 Quasi-monochromatic Light

Monochromatic light is characterized by a single temporal frequency  $\nu$ . Polychromatic light contains multiple frequencies or a spread in temporal bandwidth  $\Delta\nu$ . The finite bandwidth corresponds to a loss of temporal coherence. Some sources, such as an incandescent lamp, emit a relatively large range of wavelengths. The focus in this section is on quasi-monochromatic light, where  $\Delta\nu \ll \nu_0$ . In this case, the bandwidth  $\Delta\nu$  is much smaller than the mean, or center frequency  $\nu_0$ . Lasers are generally quasi-monochromatic sources and their partial temporal coherence characteristics are such that the effects can be noticeable or even exploited in practical applications.

Quasi-monochromatic light can be characterized by a power spectral density that describes the relative irradiance contributions of the optical frequencies. This density function is also referred to as the lineshape. Common power spectral density functions for quasi-monochromatic light include rectangular, Gaussian, and Lorentzian<sup>1,2</sup>. Here, we consider a normalized Gaussian lineshape given by

$$\hat{S}(\nu) = \frac{1}{\sqrt{\pi}b} \exp\left[-\frac{(\nu - \nu_0)^2}{b^2}\right] \quad (2.1)$$

where  $b$  is a width parameter and  $\nu_0$  is the center frequency (Hz). The integral of the normalized spectral density over all frequencies is equal to unity. When characterizing the spectral density with a single number it is common to refer to the linewidth  $\Delta\nu$ , which is a full width at half-maximum (FWHM) measure (Hz) of the spectral density function. Considering the half-maximum value for Eq. (2.1), the following can be derived:

$$b = \frac{\Delta\nu}{2\sqrt{\ln 2}} \quad (2.2)$$

A measure of the temporal coherence of the optical field is the complex degree of temporal coherence  $\gamma(\tau)$ . It is the normalized correlation of the field where  $\tau$  is the time delay between correlation samples. The normalized spectral density and complex degree of temporal coherence are linked by a Fourier transform relationship<sup>1</sup>:

$$\gamma(\tau) = \int_0^\infty S(\nu) \exp(j2\pi\nu\tau) d\nu \quad (2.3)$$

where  $S$  is defined for positive frequencies.

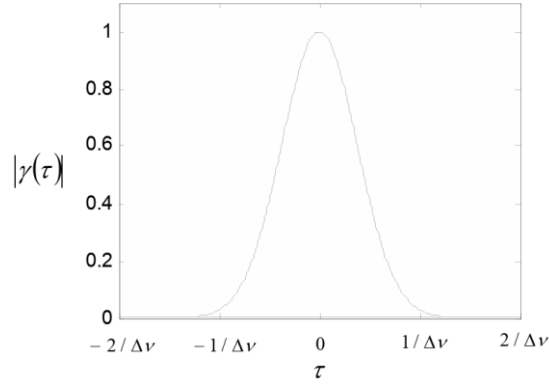


**Figure 2.1** Magnitude of the complex degree of coherence. The sign of  $\tau$  depends on which sample point is delayed.

For example, suppose  $\lambda_0 = 650$  nm and  $\Delta\nu = 2$  GHz (a wavelength and linewidth that are typical of a laser diode). In this case,  $\tau_c = 3.32 \times 10^{-10}$  s and  $l_c = 10$  cm. Imagine splitting this beam of light equally and “delaying” one part by making it travel an extra distance of 10 cm. If the two beams are recombined, the contrast in the resulting interference fringes will be low.

## 2.2 Partial temporal coherence simulation approach

For simulation purposes the total irradiance in an x–y plane can be modeled as<sup>8</sup>

$$I(x, y) = \sum_{n=0}^N S(\nu_n) I(x, y; \nu_n) \delta\nu \quad (2.4)$$

where  $n$  indexes the components,  $N$  is the number of components, and  $\delta\nu$  is the frequency interval between components.

Thus, the simulation approach is to propagate (or image with) a series of fields at different frequencies, form the irradiance for each, weigh each by the power spectral density, and sum the patterns to get the partially coherent result.

This approach ignores frequency component cross-correlations, in other words, interference between frequency components. Cross-correlation could result in temporal beating effects in the irradiance rather than a stationary pattern. The beat frequencies would be equal to the differences of the component frequencies but may not be detectable by the sensor depending on the sensor’s temporal response. The correlations may also be weak. Although not fully justified, this is a common assumption in practice that seems to give credible results.<sup>7,9</sup>

To observe partial temporal coherence effects, some type of differential delay must occur between different segments of the field in traveling from the source to the observation plane.

## 2.3 Programing for the Simulation of Partial Temporal Coherence

Consider the arrangement in Fig. 2.2. Two parallel beams, both circular in shape with radius  $w$ , enter from the left with a center-to-center separation of  $\Delta s$ . They are

assumed to have come from the same source with no temporal delay between them. Using mirrors, the lower leg takes a detour that adds a distance of  $\Delta d$  to its path relative to the top beam. This can be interpreted as a relative time delay of  $\tau = \Delta d/c$ . The beams are focused by a lens of focal length  $f$  to form a Fraunhofer pattern. This is essentially Young's double-slit arrangement, except with holes and a lens. Diffractive effects to the left of the lens are ignored, so circle functions are assumed for the beams at the lens.

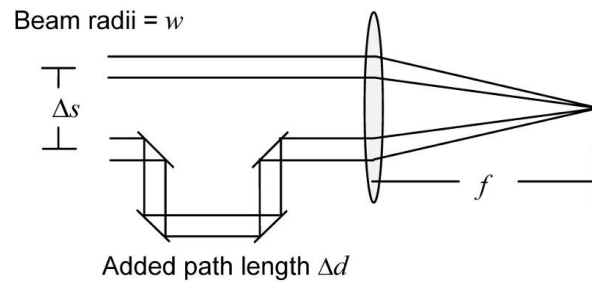


**Figure 2.2** Two-beam temporal coherence arrangement.

Choose some parameters for the simulation; for example,  $\lambda_0 = 650$  nm,  $\Delta\nu = 2$  GHz,  $w = 1$  mm,  $\Delta s = 5$  mm,  $f = 0.25$  m, and  $\Delta d = 5$  cm. Here is the code:

```
% pc_temp partial temporal coherence example
clc, clear, close all
lambda0=650e-9;    %center wavelength (m)
c=3e8;             %speed of light
k0=2*pi/lambda0;   %center wavenumber
nu0=c/lambda0;     %center frequency

% Gaussian lineshape parameters
N=51;              %number of components (odd)
delnu=2e9;         %spectral density FWHM (Hz)
b=delnu/(2*sqrt(log(2))); %FWHM scaling
dnu=4*delnu/N;     %freq interval

% source plane parameters
L1=50e-3;          %source plane side length
M=250;             %# samples (even)
dx1=L1/M;          %sample interval
x1=-L1/2:dx1:L1/2-dx1; %source coords
x1=fftshift(x1);    %shift x coord
[X1,Y1]=meshgrid(x1,x1);

% beam parameters
w=1e-3;            %radius
dels=5e-3;         %transverse separation
deld=5e-2;         %delay distance
```

```

f=0.25; %focal dist for Fraunhofer
lf=lambda0*f;

% loop through lines
I2=zeros(M);
for n=1:N
    % spectral density function
    nu=(n-(N+1)/2)*dnu+nu0;
    S=1/(sqrt(pi)*b)*exp(-(nu-nu0)^2/b^2);
    k=2*pi*nu/c;
    % source
    u=circ(sqrt((X1-dels/2).^2+Y1.^2)/w)...
        +circ(sqrt((X1+dels/2).^2+Y1.^2)/w)...
        *exp(1i*k*deld);
    % Fraunhofer pattern
    u2=1/lf*(fft2(u))*dx1^2;
    % weighted irradiance and sum
    I2=I2+S*(abs(u2).^2)*dnu;
end

I2=ifftshift(I2); %normalize/center irradiance
x2=(-1/(2*dx1):1/L1:1/(2*dx1)-1/L1)*lf; %obs coords
y2=x2;

figure(1) %irradiance image
imagesc(x2,y2,I2);
xlabel('x (m)'); ylabel('y (m)');
axis square; axis xy; colormap('gray');

figure(2) %irradiance profile
plot(x2,I2(M/2+1,:));
xlabel('x (m)'); ylabel('Irradiance');

```

Line 41: The front-end Fraunhofer phase terms are ignored. The center wavelength  $\lambda_0$  is used for scaling the Fraunhofer pattern in both the multiplicative  $1/lf$  term and the Fraunhofer coordinates  $x_2$  (line 47). The slight spread in wavelength for the quasi-monochromatic light causes insignificant effects in these terms (unlike the optical path difference term).

## 3 Partial Spatial Coherence

### 3.1 Stochastic transmission screen

The field from an ideal point source is perfectly spatially coherent. If the field from

the source is observed at two points in space, the amplitudes will be perfectly correlated. But with a spatially extended collection of independently radiating point sources involving different frequencies and amplitudes, the correlation between the field at the two observation points decreases. Similarly, if the field is somehow affected randomly in time along the different propagation paths, then spatial coherence will decrease. Conversely, as light travels a long distance from a source, the wavefront becomes more planar and spatial coherence increases. For example, light from distant stars has high spatial coherence.

A measurement of spatial coherence is the complex coherence factor  $\mu_{12}$ . It is a normalized correlation of the field at two points, 1 and 2. We are concerned with  $|\mu_{12}|$ , where it can be shown that

$$0 \leq |\mu_{12}| \leq 1$$

The correlation between the field samples is performed over time. Suppose the two points are separated in the x–y plane by the values  $x'$  and  $y'$ , respectively. For simulation purposes we consider a simple model with a deterministic part of the field  $U_0(x, y)$  and a stochastic temporal component introduced through a complex transmittance screen  $t_A(x, y; t)$ . Thus, the field is modeled by

$$U(x, y; t) = U_0(x, y)t_A(x, y; t) \quad (3.1)$$

A quantity of interest is the time-averaged spatial autocorrelation function of the transmittance screen, given as

$$R(x', y') = \langle t_A(x + x', y + y'; t)t_A^*(x, y; t) \rangle \quad (3.2)$$

A commonly used form for the spatial correlation function is a Gaussian

$$R(x', y') = \exp\left(-\frac{x'^2 + y'^2}{l_{cr}^2}\right) \quad (3.3)$$

### 3.2 Partial spatial coherence simulation approach

The simulation approach is outlined as follows: a spatially random transmittance screen is applied to a deterministic beam field, the result is propagated, and the irradiance is formed. The process is repeated many times with different realizations of the screen and the resulting irradiance patterns are averaged to produce the partial spatial coherent result. The procedure is illustrated in Fig. 3.1.

A convenient form of a transmittance function is a complex phasor given by

$$t_A(x, y) = \exp(j\phi(x, y)) \quad (3.4)$$

where  $\phi(x, y)$  is a spatially correlated, random phase function that is often called a phase screen.

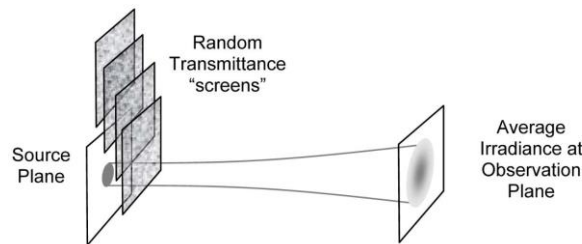


**Figure 3.1** Illustration of partial spatial coherence simulation approach.

The Gaussian correlation function is obtained in formular (3.3), where the transverse coherence length is given by

$$l_{cr}^2 = \frac{4\pi\sigma_f^4}{\sigma_r^2} \quad (3.5)$$

then using the property of a linear filter with a random input signal we write<sup>11</sup>

$$|\Phi(f_X, f_Y)|^2 = \sigma_r^2 |F(f_X, f_Y)|^2 \quad (3.6)$$

So, the computational approach to get a random realization of  $\phi$  is to fill an array with random values  $r(p, q)$ , multiply by  $\sigma_r/\Delta f_x$ , multiply by the filter response  $F$ , and take the inverse FFT.

One final trick is to make  $r(p, q)$  random complex array, where the real and imaginary parts are independent Gaussian random values.

### 3.3 Programing for the Simulation of Partial Spatial Coherence

To illustrate partial spatial coherence effects, the same optical arrangement as for the temporal case is used, but the path delay is removed. In this case the limited spatial coherence does the job of reducing the fringe contrast in the Fraunhofer pattern. The same parameters as in the temporal case are used for the simulation:  $\lambda = 650$  nm,  $w = 1$  mm,  $\Delta s = 5$  mm, and  $f = 0.25$  m. The transverse coherence length is selected as  $l_{cr} = 8$  mm, which is on the order of  $\Delta s$  and, therefore, should produce an obvious reduction in coherence between the two beams. In this case,  $|\mu_{12}| = 0.677$

```
% pc_spatial partial spatial coherence example
clc, clear, close all
lambda=650e-9;      %center wavelength (m)

L1=50e-3;           %source plane side length
M=250;              %# samples (even)
dx1=L1/M;           %sample interval
x1=-L1/2:dx1:L1/2-dx1; %source coords
x1=fftshift(x1);     %shift x coord
[X1,Y1]=meshgrid(x1,x1);

% beam parameters
w=1e-3;             %radius
dels=5e-3;          %transverse separation
f=0.25;             %Fraunhofer focal distance
lf=lambda*f;

% partial spatial coherence screen parameters
N=100;              %number of screens (even)
Lcr=8e-3;           %spatial correlation length
sigma_f=2.5*Lcr;     %Gaussian filter parameter
sigma_r=sqrt(4*pi*sigma_f^4/Lcr^2); %random std
```



```

dfx1=1/L1;
fx1=-1/(2*dx1):dfx1:1/(2*dx1)-dfx1;
fx1=fftshift(fx1);
[FX1,FY1]=meshgrid(fx1,fx1);

% source field
u1=circ(sqrt((X1-dels/2).^2+Y1.^2)/w)...
    +circ(sqrt((X1+dels/2).^2+Y1.^2)/w);
% filter spectrum
F=exp(-pi^2*sigma_f^2*(FX1.^2+FY1.^2));

% loop through screens
I2=zeros(M);
for n=1:N/2
    % make 2 random screens
    fie=(ifft2(F.*(randn(M)+1i*randn(M)))...
        *sigma_r/dfx1)*M^2*dfx1^2;
    % Fraunhofer pattern applying screen 1
    u2=1/lf*(fft2(u1.*exp(1i*real(fie))))*dx1^2;
    I2=I2+abs(u2).^2;
    % Fraunhofer pattern applying screen 2
    u2=1/lf*(fft2(u1.*exp(1i*imag(fie))))*dx1^2;
    I2=I2+abs(u2).^2;
end

I2=ifftshift(I2)/N; %normalize & center irradiance
x2=(-1/(2*dx1):1/L1:1/(2*dx1)-1/L1)*lf; %obs coords
y2=x2;

figure(1) %irradiance image
imagesc(x2,y2,I2);
xlabel('x (m)'); ylabel('y (m)');
axis square; axis xy;
colormap('gray');

figure(2) %irradiance slice
plot(x2,I2(M/2+1,:));
xlabel('x (m)'); ylabel('Irradiance');

```

Line 39: The random number generator `randn` creates an array of zero-mean normally distributed random values. Scaling the phase function  $\phi(x,y)$  appropriately requires several factors:  $/dfx1$  comes from Eq. (3.6.);  $M^2$  counteracts the  $1/MN$  factor that accompanies the `ifft2` function;  $dfx1^2$  is applied to correctly approximate the inverse Fourier transform integral.

## 4 Reducibility, Number of Spectral Components

Temporal and spatial coherence are treated separately in the developments of the previous sections. However, the general form of the complex degree of coherence  $\gamma_{12}(\tau)$  encompasses both temporal and spatial field correlations and can include cross-correlations of the frequency components. Coherence separation implies  $\gamma_{12}(\tau)$  can be factored into a temporal term and spatial term product, or<sup>1</sup>

$$\gamma_{12}(\tau) = \mu_{12}\gamma(\tau) \quad (4.1)$$

## 5 Reference

1. B. E. A. Saleh and M. C. Teich, Fundamentals of Photonics, 2nd Ed., Wiley Interscience, New York (2007).
2. E. Hecht, Optics, 4th Ed., Addison-Wesley, Reading, MA (2002).
3. K. K. Sharma, Optics: Principles and Applications, Academic, London (2006).
4. J. W. Goodman, Introduction to Fourier Optics, 3rd Ed., Roberts & Company, Greenwood Village, CO (2005).
5. C. Rydberg and J. Bengtsson, "Efficient numerical representation of the optical field for the propagation of partially coherent radiation with a specified spatial and temporal coherence function," J. Opt. Soc. Am. A, 23, 1616–1625 (2006).
6. J. W. Goodman, Statistical Optics, Wiley-Interscience, New York (1985).
7. L. Mandel and E. Wolf, Optical Coherence and Quantum Optics, Cambridge
8. D. G. Voelz, K. A. Bush, and P. S. Idell, "Illumination coherence effects in laser-speckle imaging: Modeling and experimental demonstration," Appl. Opt., 36, 1781–1788 (1997).
9. P. Polynkin, A. Peleg, L. Klein, T. Rhoadarmer, and J. Moloney, "Optimized multiemitter beams for free-space optical communications through turbulent atmosphere," Opt. Lett., 32, 885–887 (2007).
10. X. Xiao and D. Voelz, "Wave optics simulation approach for partial spatially coherent beams," Opt. Express, 14, 6986–6992 (2006).
11. A. Papoulis and S. Unnikrishna Pillai, Probability, Random Variables, and Stochastic Processes, 4th Ed., McGraw-Hill, New York (2002).
12. H. A. Makse, S. Havlin, M. Schwartz, and H. E. Stanley, "Method for generating long-range correlations for large systems," Phys. Rev. E, 53, 5445–5449 (1996).
13. J. C. Ricklin and F. M. Davidson, "Atmospheric optical communication with a Gaussian Schell beam," J. Opt. Soc. Am. A, 20, 856–866 (2003).